Delft University of Technology

Improving Patient Comfort in MRI with Predictive Acoustic Noise Cancelling

Siuryte, Paulina; Tourais, Joao; Weingartner, Sebastian

Citation (APA)
Siuryte, P., Tourais, J., & Weingartner, S. (2022). Improving Patient Comfort in MRI with Predictive Acoustic Noise Cancelling. In *2022 44th Annual International Conference of the IEEE Engineering in Medicine and Biology Society* (Vol. 2022, pp. 1468-1471). IEEE. https://doi.org/10.1109/EMBC48229.2022.9871344

Important note
To cite this publication, please use the final published version (if applicable).
Please check the document version above.

Improving Patient Comfort in MRI with Predictive Acoustic Noise Cancelling*

Paulina Šiurytė[1], Joao Tourais[1] and Sebastian Weingärtner[1,2]

Abstract— With sound pressure levels reaching up to 130 dB, acoustic noise in Magnetic Resonance Imaging (MRI) is one of the main sources of patient discomfort in otherwise one of the safest medical imaging modalities. In this work, a noise prediction-based approach, termed predictive noise cancelling (PNC), is applied, for the first time, to suppress noise in MRI. In PNC the noise from the scanner gradient coils is predicted based on linear time-invariant models, which relate the individual gradient coil (X, Y and Z) input to the acoustic noise output. A model setup was constructed of a custom speaker box and MRI-compatible microphone to demonstrate live noise reduction. Additional tuning steps, including output channel equalization and clock mismatch correction, were performed to maximize noise reduction. A calibration sequence was designed to determine the model and tuning parameters. Analysis of actual scanner noise shows an upper limit of 21 dB noise reduction with the proposed linear model. For the components of a clinical example sequence, the setup demonstrated in-bore live noise reduction of up to 10 dB (7.01 ± 0.31 dB, 6.42 ± 2.04 dB and 9.28 ± 0.26 dB for X, Y and Z gradient coils respectively) in the presence of system imperfections.

Clinical relevance— The results indicate promising noise attenuation without the need to modify scanner hardware or compromises in acquisition speed or quality. This has potential to substantially and cost effectively improve patient comfort in clinical MRI.

I. INTRODUCTION

Acoustic noise in Magnetic Resonance Imaging (MRI) is a major contributor to patient discomfort, with sound pressure levels (SPL) reaching up to 130 dB during a scan [1], [2]. The noise is largely caused by rapid switching of the gradient coil system during an MRI sequence, which is necessary for spatial encoding of the image [3]. During the switching, as the current passed through the coils rapidly changes, Lorentz forces induce audible coil vibrations.

To alleviate the noise burden, common practice in clinical settings is to use passive noise cancelling with earplugs and/or headphones. These techniques achieve 10-30 dB attenuation and allow to bring the exposure closer the safety zone of below 85 dB [4]. Alternatively, "silent MRI" scanning has been proposed [5]. Here MRI sequences are modified to limit coil vibrations by switching gradients more slowly. This approach, however, limits the achievable image quality and prolongs scan time. Silent MRI gradient systems have also been proposed, e.g. by mounting the gradient coils in vacuum [6]. Hardware solutions, however, are very cost intensive and usually only available in top line scanners.

Active noise cancelling (ANC) has been explored, to reduce the MRI noise burden independently of the scanner hardware [7]. In ANC, adaptive algorithms use microphone input to predict sound in the next immediate time step. An opposite phase sound, called anti-noise, is then calculated and applied in real time to minimize the superimposed sound wave pressure. Most ANC setups in MRI have been limited by the necessity to place electronics outside the scanner, which restricts the real-time application due to extended signal travel time [7]. Present ANC approaches record the sound of a repetitive sequence, to generate a predefined anti-noise signal, which can be played back at future sequence repetitions. This restricts the use to a small set of repetitive applications, such as functional MRI studies [8]. In the clinic, however, patient scans comprise a wide range of different scan protocols, preventing the use of this approach [9].

In this work, we present a new approach, called predictive noise cancelling (PNC). To circumvent the issue with travel time between speakers and the in-bore sound wave in PNC, anti-noise is generated from a prediction based on the gradient coil inputs prior to sequence starting. We describe a cost-efficient model setup for live noise cancelling and evaluate its potential for noise reduction for various MRI sequences, in silico and in live in-bore experiments.

II. METHODS

A. Noise cancelling setup

A model of the noise cancelling setup was constructed, consisting of a microphone and a speaker inside the bore, as well as supporting hardware outside the scanner room. A custom-made wooden speaker box was positioned in the control room and a rubber hose was attached to channel the gathered sound inside the bore, see Fig.1. The speaker box consisted of two parts, with 25 cm diameter woofer installed on a left side cushioned with a sound-isolating material and installing external plugs for an amplifier connection. On the right side, a sound-gathering plastic funnel was placed to cover the woofer. The narrow end of the funnel measured 35 mm in diameter, matching that of the attachable hose, ≈7 m in total length. At the other end of the hose, a widening plastic funnel was attached using silicon.

An optical fiber microphone was used (Phonoptics, France), with its conditioning unit placed in the control room. All signals were recorded and processed with a PC using LabVIEW (National Instruments, Austin, TX, USA) and Matlab (MathWorks, Natick, MA, USA). For generating time-synchronised signals, an arbitrary function generator (AFG, AFG31002, Tektronix, Beaverton, OR, USA) was
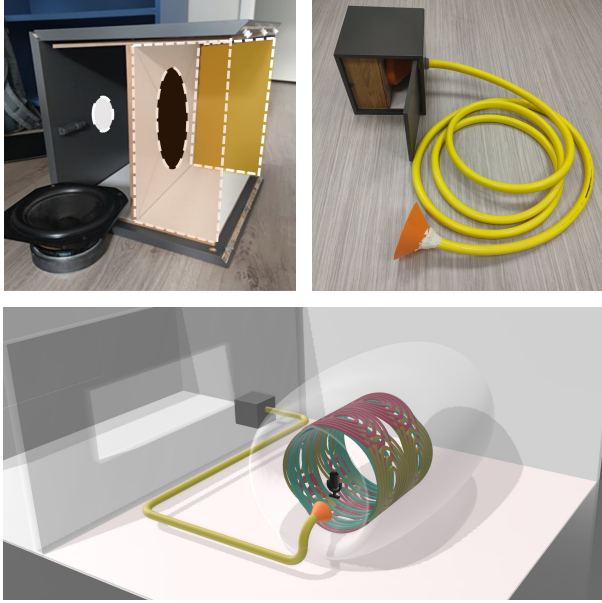
Fig. 1. Experimental PNC setup. Top left image shows the speaker box during construction. The box and hose attachment are shown on the top right image. During the experiments, the speaker box is placed in the control room while the other end of the hose is placed inside the MRI bore (bottom).

used and operated through LabVIEW. Once in noise cancelling mode, the sound output is triggered by a timed gradient pulse noise from the scanner. Upon detecting the trigger the microphone sends a trigger input to the AFG operating in the positive slope trigger mode.

All signals were recorded at 44.1 kHz sampling rate and band-pass filtered to 0.3 - 6 kHz. The lower frequency filter limit was determined by the continuous background noise from the helium pump, which is periodic, but not coupled to the MRI sequence execution, and therefore is not part of the anti-noise prediction. The higher filter limit was chosen based on the extent of a typical gradient noise spectrum.

B. Linear time-invariant model

Acoustic noise $p_{x/y/z}(t)$ caused by each gradient coil can be modelled as a linear time-invariant system, observing a direct link between the gradient coil current input $g_{x/y/z}(t)$ derivative, $g'_{x/y/z}(t)$, and resulting sound via system transfer function $h_{x/y/z}(t)$ [10]. This linearity can be expressed in frequency domain as

$$P_{x/y/z}(f) = H_{x/y/z}(f) \cdot G'_{x/y/z}(f), \tag{1}$$

where $H_{x/y/z}(f)$ represent measured system transfer functions [2], [11], [12]. In PNC $H_{x/y/z}(f)$ are determined from a set of calibration pulses and corresponding noise output. Once the transfer functions are known, anti-noise for a regular MRI sequence is predicted based on the gradient coil inputs described in the pulse sequence diagram.

C. Output tuning

For effective noise reduction, precise timing and output frequency spectrum fidelity are crucial. In the constructed

setup, three output corrections are made to achieve this:

1) Signal latency calibration is needed to ensure the timing between the acoustic trigger reception and output sound is tuned. Due to the time it takes for the sound to travel through the system, and an unknown exact acoustic trigger threshold, latency can vary for each scan session. A scanner pulse can be used as an acoustic trigger. Followed by either another scanner pulse, or triggering a pulse noise prediction sound, this combination allows to estimate the total system latency. This is done by comparing the time delays between the scanner sound and the trigger or the output sounds and the trigger.

2) Clock mismatch between the recording device and the scanner causes the sound and anti-noise to go out of phase over time. To accurately estimate this mismatch and re-sample the recorded signals, a long reference MRI sequence with periodic noise is used. By comparing the time periods in recorded signals (PC time) and MRI input sequence diagrams (scanner time) the average clock shift per second can be identified.

3) Distortion introduced by the speaker-hose system to the sound requires correction via channel equalization, to achieve the desired anti-noise signal at the in-bore location. In order to correct the distortion, the input $p_i(t)$ and output $p_o(t)$ are assumed to also form a linear time-invariant system, connected via channel-distortion filter $h_{cd}(t)$, as $p_o(t) = p_i(t) * h_{cd}(t)$. For p_o to approach p_i, the input is convolved with a calculated inverse filter $h_{EQ} \approx h_{cd}^{-1}$. A dummy AFG input signal and a recorded playback through the speaker, is used to estimate the inverse channel filter.

D. Calibration sequence

All in bore experiments were performed with a Philips Ingenia 3T system (Philips, the Netherlands) at HollandPTC (Delft, Netherlands). A calibration sequence was designed, in order to calculate the required transfer functions $H_{x/y/z}(f)$ and obtain the tuning information listed above. The 1 min sequence consists of a series of triangular gradient pulses played on all three gradient coils with a 0.14 ms rise time and 20 mT/m amplitude. 20 such blips are played out with a 3 s repetition time (TR), and used as a time reference point (see Fig.2, black pulses). During the sequence, these pulses are followed by a single-gradient triangular pulse on the scanner (colored pulses in Fig.2). Averaged pulses were then used to estimate $H_{x/y/z}(f)$ as in Eqn.1.

To estimate the absolute latency, the same sequence was repeated but with single gradient pulses played not on the scanner but as a noise prediction. The time delay compared to the scanner pulses was used to tune the latency.

The clock mismatch was calculated from the train of time reference gradient pulses. In the PC recordings, they gradually shift from the expected 3 s repetition time.

Finally, the equalizer filter h_{EQ} was estimated by calculating an inverse transfer function for input/output pair of the
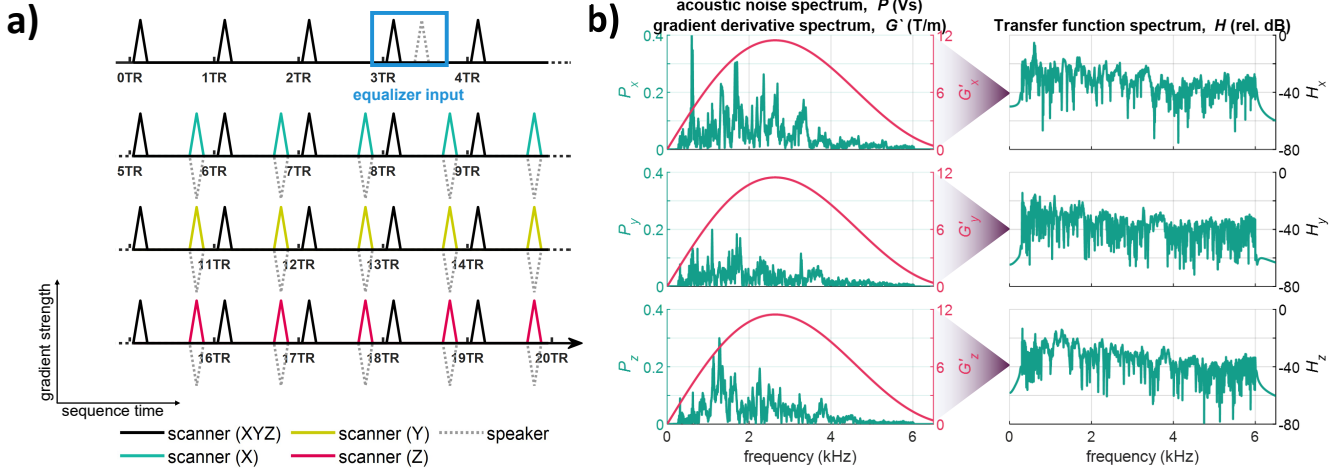
Fig. 2. Calibration sequence scheme (a) and transfer function derivation (b). All calibration pulses have 20 mT/m amplitude and 0.14 ms rise time. Acoustic trigger pulses, indicated in black, are played out on all 3 coils simultaneously. Colored pulses represent single-gradient scanner pulses used to derive the transfer functions, while dashed lines under those indicate an anti-noise in the last calibration step. Equalizer inputs are indicated in a blue area, where the dashed pulse shows a speaker playback of the recorded trigger pulse. In (b), the transfer functions are estimated via $H_{x/y/z}(f) = P_{x/y/z}(f)/G'(f)$. Calibration pulse noise $P_{x/y/z}(f)$ is illustrated on the left (teal), along with a gradient derivative $G'(f)$ of a triangular pulse (pink). Corresponding transfer function frequency spectra are plotted in relative dB scale on the right.

scanner gradient pulse noise p_i and a record of a playback noise p_o. This is indicated in blue in Fig.2, (a).

E. Noise reduction experiments

In order to evaluate the effect of experimental error sources and estimate the maximum noise reduction possible with the linear model, simulated noise experiments were performed. Here perfect timing and frequency channel equalization was assumed. Thus, the simulated SPL reduction only reflects the accuracy of the sound representation by the linear model.

Two live noise reduction experiments were performed in total. The prediction was first applied to the single-gradient triangular pulses, which had the same parameters as in the above calibration sequence. Secondly, an example clinical MRI sequence gradient component noise was reduced.

During the triangular gradient pulse experiment, a train of acoustic triggers as in calibration sequence is employed, followed by single gradient triangular pulses. Each pulse noise reduction is acquired with 5 averages (see Fig.2, (a)).

A regular MRI sequence, spoiled gradient-echo (GRE), was chosen with TR = 10.6 ms and ≈11 s duration. The sequence on the scanner was preceded by previously described acoustic trigger pulse, which was used as a synchronization point for signal-processing and anti-noise. Live anti-noise experiments were acquired with 6 averages for each coil.

III. RESULTS

A. Calibration sequence

Averaged calibration pulse noise $P_{x/y/z}(f)$, gradient input derivative $G'(f)$ envelope and the derived transfer function $H_{x/y/z}(f)$ frequency spectra are shown in Fig.2, (b).

During calibration a clock mismatch of 12.2 μs per second was measured and used to re-sample all recorded signals.

B. Triangular gradient pulses

For the triangular pulses, the model limit from simulations was estimated as 21.65, 21.04 and 22.91 dB reduction for X, Y and Z coils.

In live experiments good noise reduction was found for all tested gradient configurations. Lower reduction as compared to the model limit was found, indicating substantial contributions for error source: 7.16 ± 0.17 dB, 8.27 ± 0.38 dB and 7.29 ± 0.14 dB noise reduction was found in live experiments for X, Y and Z coils respectively.
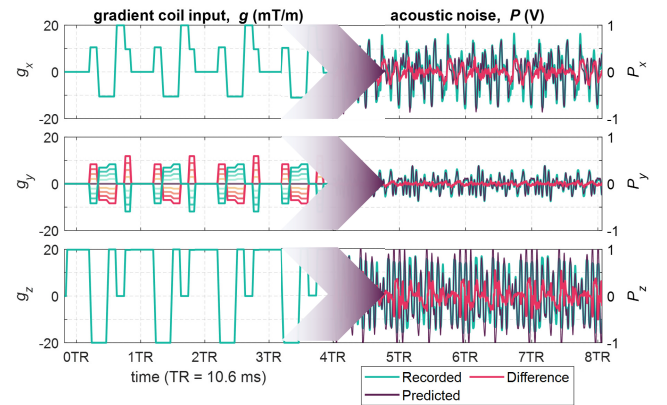

Fig. 3. Spoiled GRE sequence gradient inputs (left). Measurement gradient was arbitrarily assigned to X coil, phase gradient to Y coil and slice selection gradient to Z coil. The corresponding noise prediction along with the original and the attenuated sequence noise is also shown (right). Sequence TR/TE = 10.6/6.4 ms ant total length ≈11 s

C. Regular MRI sequence

For a spoiled GRE sequence, the estimated maximum reduction with the linear model from the simulations was 9.99 dB, 13.52 dB and 9.85 dB for X,Y and Z coils

respectively. Experimentally, this translated to mean values of 7.01 ± 0.31 dB, 6.42 ± 2.04 dB and 9.28 ± 0.26 dB reduction. An example acquisition of the acoustic signal power before and after the application of predictive noise cancelling is illustrated in Fig.4.

IV. DISCUSSION

In this study we have demonstrated the feasibility of predictive noise cancelling to alleviate the noise burden in MRI scanning. With an example in-house built, low-cost system for MRI-compatible PNC, up to 10 dB noise reduction was demonstrated, in live in-bore experiments. The principle was demonstrated for GRE sequence, however, the principle is applicable to any MRI gradient combination, and other sequences are to be investigated in the future.

The difference between the estimated model limit and the actual measured noise reduction in both calibration and regular sequences illustrate the extent of experimental error sources. The equalizer is likely the main contributor to the signal imperfection. Thus, advanced equalizers, or iterative equalization can be applied for further improved channel correction. Alternatively, MRI-compatible speakers with high fidelity can be employed and placed in the scanner room, to minimize channel distortion. This will be explored in future studies to further improve noise attenuation with PNC.

Another contributor preventing higher reduction is background noise, which includes periodic helium pump noise, as well as ventilation and other systems. In order to reduce its' effect on derived transfer function accuracy, noise source separation could be used in the future.

PNC can also be combined with passive noise cancelling as presently used in clinical MRI. PNC is more effective in lower frequencies as it is less prone to dephasing, while passive noise cancelling is more effective in higher frequencies, as it can be attenuated with padding compatible with the spatial constraints. A headphone setup with integrated microphones, as commonly used for acoustic fMRI experiments, can be explored to evaluate the full attenuation potential of a joint approach. Furthermore, additional attenuation in the lower frequency range can be achieved by including the periodic helium pump sound into the prediction, although this noise source is weak compared to the gradient coils.

V. CONCLUSION

First experiments with predictive noise cancelling show promising active noise attenuation. Despite system imperfections, up to 10 dB noise reduction was presented based on a linear time-invariant prediction model in live in-bore experiments. Future, optimized setups may achieve even higher attenuation, up to the model limitations of around 20 dB. Therefore, PNC bears great promise as a cost effective solution to improve patient comfort without the need for new or modified scanner hardware.

ACKNOWLEDGMENTS

The authors would like to thank the remainder of the MarsLab, as well as Christal van de Steeg-Henzen for additional support with setting up the experiments.
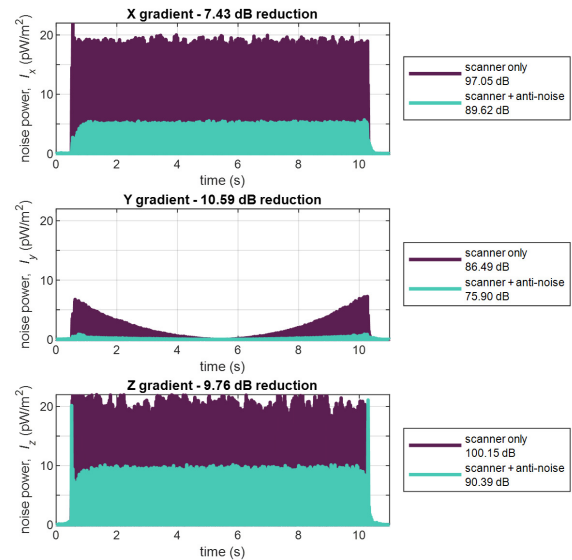

Fig. 4. Live spoiled GRE sequence noise reduction results. Sound intensities are plotted for scanner sequence components (blue) and for scanner noise with simultaneous anti-noise output (pink). Up to 90% signal intensity reduction is shown. The reference intensity used was $I_0 = 1 \mathrm{pW/m^2}$

REFERENCES

[1] More SR, Lim TC, Li M, Holland CK, Boyce SE, Lee JH. Acoustic noise characteristics of a 4T MRI scanner. J Magn Reson Imaging 2006;23: 388-397.

[2] S. R. More, T. C. Lim, M. Li, C. K. Holland, S. E. Boyce, J. H. Lee. Acoustic noise characteristics of a 4 Telsa MRI scanner. Journal of Magnetic Resonance Imaging, 2006;23(3), 388-397.

[3] S. Hidalgo-Tobon. Theory of gradient coil design methods for magnetic resonance imaging. Concepts Magn. Reson., 2010;36A: 223-242.

[4] M. J. McJury Acoustic Noise and Magnetic Resonance Imaging: A Narrative/Descriptive Review. Journal of Magnetic Resonance Imaging, 2021.

[5] M. Segbers, C. V. R. Sierra, H. Duifhuis, J. M. Hoogduin. Shaping and timing gradient pulses to reduce MRI acoustic noise. Magnetic resonance in medicine, 2010;64(2), 546-553.

[6] A. Katsunuma, H. Takamori, Y. Sakakura, Y. Hamamura, Y. Ogo, R. Katayama. Quiet MRI with novel acoustic noise reduction. Magnetic Resonance Materials in Physics, Biology and Medicine, 2001;13(3), 139-144.

[7] M. McJury, et al. The use of active noise control (ANC) to reduce acoustic noise generated during MRI scanning: some initial results. Magnetic resonance imaging 1997; 15.3: 319-322.

[8] Optoacoustics, OptoActive II.https://www.optoacoustics.com/medical/optoactive-ii Accessed on January 24, 2022.

[9] A. Martinez-Möller , M. Eiber, S.G. Nekolla, et al. Workflow and scan protocol considerations for integrated whole-body PET/MRI in oncology. Journal of Nuclear Medicine. 2012 1;53(9):1415-26.

[10] R. A. Hedeen and W. A. Edelstein. Characterization and prediction of gradient acoustic noise in MR imagers. Magnetic Resonance in Medicine, 1997;37(1), 7-10.

[11] C. V. R. Sierra, M. J. Versluis, J. M. Hoogduin, H. Duifhuis. Acoustic fMRI noise: linear time-invariant system model. IEEE Transactions on Biomedical Engineering, 2008;55(9), 2115-2123.

[12] Z. Wu, Y. C. Kim, M. C. Khoo, K. S. Nayak. Evaluation of an independent linear model for acoustic noise on a conventional MRI scanner and implications for acoustic noise reduction. Magnetic Resonance in Medicine, 2014;71(4), 1613-1620.